# Data Acquisition and Health Analysis of In-service Railway Vehicle for Structural Health Monitoring

LEI ZU, CHANG PENG, LONG MA, SHI-PING GAO, PING-YU ZHOU, BUZHAO NIU, FRANKLIN LI and AMRITA KUMAR

## ABSTRACT

The enormous number of trains, increasing operation speeds, and complex line environments places greater urgency on ensuring the service safety of rail vehicle structures. This paper focuses on the application of structural health monitoring techniques to perform online monitoring of rail vehicle structural components. An onboard monitoring system was designed and installed, which uses piezoelectric sensors to perform ultrasonic guided wave acquisition, temperature compensation, and damage detection in a particular area during an online tracking test. Ultrasonic guided waves are affected by temperature and stress/loading conditions. The damage indices after temperature compensation change rapidly at different stations and different positions of the railway line, which may be affected by passenger load or line conditions, but remain at a low level after the train has entered the warehouse. The results show that the system can adapt to the railway line environment and automatically collect ultrasonic guided wave data that can be used to assess damage.

## INTRODUCTION

By the end of 2020, China's railway business mileage was 146,300 kilometers, including 38,000 kilometers of high-speed railway and 76,000 railway passenger cars, among which are 3,918 EMUs and 31,340 standard units [1]. The enormous number of trains makes overhaul and maintenance a challenge. The combination of online monitoring and the "five-level maintenance" system fully ensures the operation safety of trains in service; however, with continuously increasing running speed, the load that is borne and transmitted between wheel and rail increases, the vehicle vibration intensifies, the possibility of hunting instability increases, the vibration and noise increases, and comfort and stability are reduced [2].

---

Lei Xu, Chang Peng, Long Ma, Shi-ping Gao, Ping-yu Zhou, Buzhao Niu, CRRC Qingdao Sifang Co., Franklin Li, Amrita Kumar, Acellent Technologies Inc.

Meanwhile, the service environment of key bearing components (such as carbody, bogie, and vehicle installation equipment) deteriorates, the amplitude and frequency of variable load increase, the instantaneous impact load becomes higher, and the fatigue reliability and safety decrease. Worse, the train operates in different geographical and climatic environments (such as plains, hills, mountains, and plateaus) and bears the effects of significantly different temperatures, humidity, wind, sand, rain, and snow along the railway line [3]. Especially in coastal environments and those with higher levels of acid rain and SO2, the vehicle structure experiences continuous erosion, which may lead to stress corrosion and other failures.

The introduction of structural health monitoring (SHM) into train systems can be regarded as a supplement and improvement to online monitoring (currently mainly monitoring vehicle operation status). By collecting signals representing the train's structural status and evaluating its health status, SHM can maximize the service safety of vehicles and transition from the current "planned repair" model to "condition-based maintenance". SHM is widely applied in many industries, including for monitoring bridges, buildings, and aircraft. For example, the deformation, localized strain, and suspender tension on bridges are obtained by monitoring of environmental load, and the overall and local response of the structure are used to evaluate the safety level of the bridge [4]. On aircraft, advanced structural health monitoring systems are integrated into the structure to obtain its health status (such as stress, strain, temperature, damage, etc.) in real-time. By combining advanced information processing methods and mechanical modeling methods, SHM systems extract characteristic parameters and identify structural status and faults in order to provide continuous monitoring of structural status, improve structure design, and implement the "condition-based maintenance" strategy [5]. The means of obtaining data in different fields are not the same. Bridges, buildings, tunnels, mines, oil pipelines, pressure vessels, etc. are usually in a static state (which reduces concerns about the added weight of a monitoring system) and there is either no stress concentration or the degree of stress concentration is at a low level. Sensors with a certain weight and volume can be used to obtain parameters such as load, vibration acceleration in those fields. However, aircraft and trains are in the high-speed state (which requires lightweight monitoring systems), the areas of concern are generally those with high stress concentration (which requires soft, lightweight sensors), and the sensors must be tightly integrated with the structure without affecting the performance of the structure itself. Examples of suitable sensors include fiber Bragg gratings and thin piezoelectric ceramic discs, which can formed into a sensor network. Piezoelectric sensors in particular can be easily integrated with the structure by embedding them in a 0.12mm thick polyimide film [6] and bonding the film onto the surface or embedding it inside of the structure like a layer of skin.

The principles and method of using a piezoelectric sensor network to provide active monitoring of damage is well-described in a plate structure [7]. Zheng Yuebin reviewed the research progress of damage diagnosis imaging technology based on ultrasonic guided wave and compared the application scope, advantages, and disadvantages of these imaging algorithms [8]. Liang Jianying put forward the block structure surface damage monitoring method based on Rayleigh waves [9], Ju Zengye designed the piezoelectric smart sensing network of aluminum alloy carbody bolster of the train [10], Wang Qiang developed and verified the damage monitoring method for the bogie frame of the train based on the guided-wave method [11], and Xiao Junchen conducted

application research on the bogie frame using a damage location imaging method based on probability density [12]. These studies laid a foundation for the application of structural health monitoring technology to rail vehicles.

Focusing on the online monitoring requirements of structural integrity (e.g., detection of cracks, corrosion, and other damages) for key bearing components on high-speed trains, this paper describes a structural health monitoring system based on piezoelectric ultrasonic guided wave transducers, collects ultrasonic guided wave signals representing the structural status, carries out data processing and detailed analysis, extracts characteristic parameters, evaluates structural health status, and demonstrates the possibility for optimizing maintenance cycles and transitioning from "planned repair" to "condition-based maintenance".

## DESIGN AND INSTALLATION OF ONBOARD STRUCTURAL HEALTH MONITORING SYSTEM

An onboard structural health monitoring system to perform piezoelectric ultrasonic guided wave damage monitoring, including data-acquisition (DAQ) hardware and sensor network (SMART Layer®) as shown in Figure 2, was designed by Acellent Technologies, Inc. The DAQ (onboard host) includes signal generation, high-speed data acquisition, control, and storage modules. The control and storage module controls the signal generator to send out a five-peak sine wave and apply it to PZT through power amplification and channel selection; at the same time, the voltage signal of PZT is captured and stored through program-controlled amplification, bandpass filtering, and analog-to-digital conversion modules. The temperature acquisition module sends the temperature sensor data to the control and storage module.

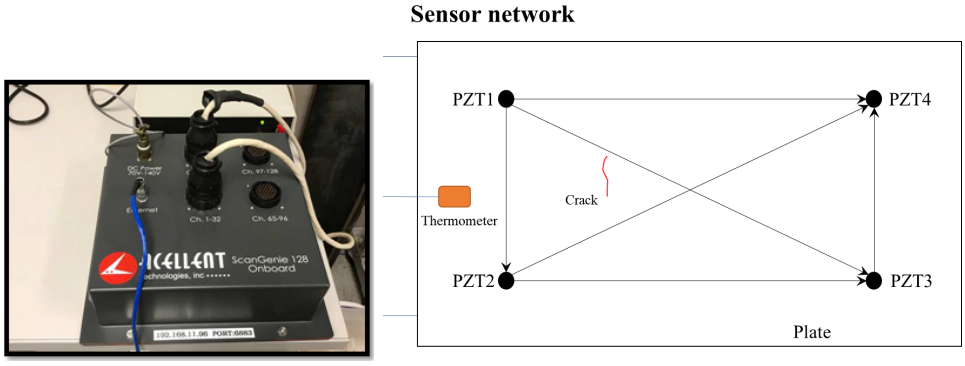


Figure 2. Schematic diagram of onboard structural health monitoring system, including onboard host (data-acquisition hardware) and sensor network (SMART Layer®), both courtesy of Acellent Technologies

One train is selected for the long-term tracking test. As shown in Figure 3, the onboard structural health monitoring system is installed on vehicle 3 and vehicle 13. According to the previous finite element simulation results, there is a stress concentration near the weld toe of the carbody bolster, so the sensor network is installed near the stress concentration areas, as shown in Figure 4. The onboard host (DAQ) is installed on the underframe beam in the equipment cabin and connected with the sensor network via cable connection. All components (SMART Layer® sensors, DAQ hardware, and software) are provided by Acellent Technologies, Inc.

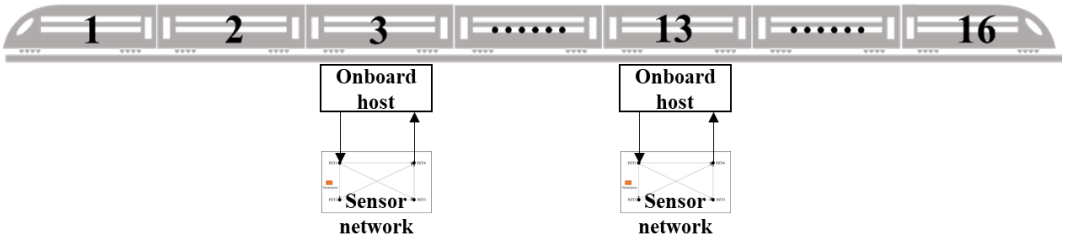


Figure 3. Installation of onboard structural health monitoring system

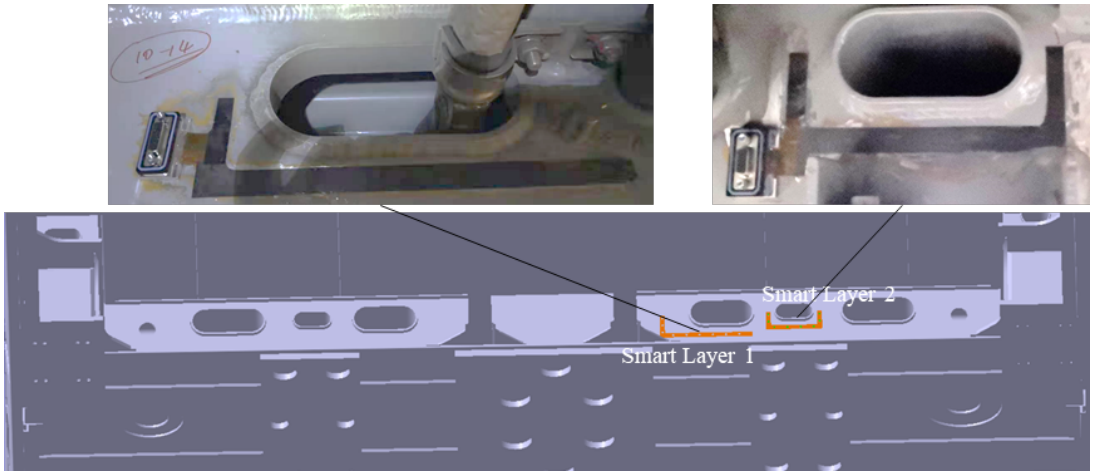


Figure 4. SMART Layer® sensor network installation location and photos

Figure 5. Piezoelectric guided wave signal data acquisition equipment

The train supplies 110 VDC power to the onboard host. Whenever the train supplies power, the onboard host automatically starts to collect and save data. The driving frequency is 350 kHz, the sampling frequency is 48 MHz, the sampling time is 1 s, and the sampling interval is 5 min. The data acquisition equipment is shown in figure 5.

## HEALTH ANALYSIS METHOD BASED ON ULTRASONIC GUIDED WAVES

After the onboard structural health monitoring system is installed on the train and collecting data, data processing and analysis are carried out. Figure 6 shows the damage analysis process using the baseline data compensation method. The initial step is to collect a baseline, which consists of ultrasonic guided wave data for a pristine (undamaged) structure covering a broad range of operational temperatures. During monitoring, an incoming data set is selected, the first arrival wave packet is located (recording its start and end time), and the damage index (DI) is calculated relative to the baseline. If the DI is less than the configured threshold (indicating an undamaged structure) and the baseline data pool does not include the current temperature, then the

current ultrasonic guided wave and temperature data are added to the baseline data library; if the DI is greater than or equal to the configured threshold, then the damage is located and its size is estimated.

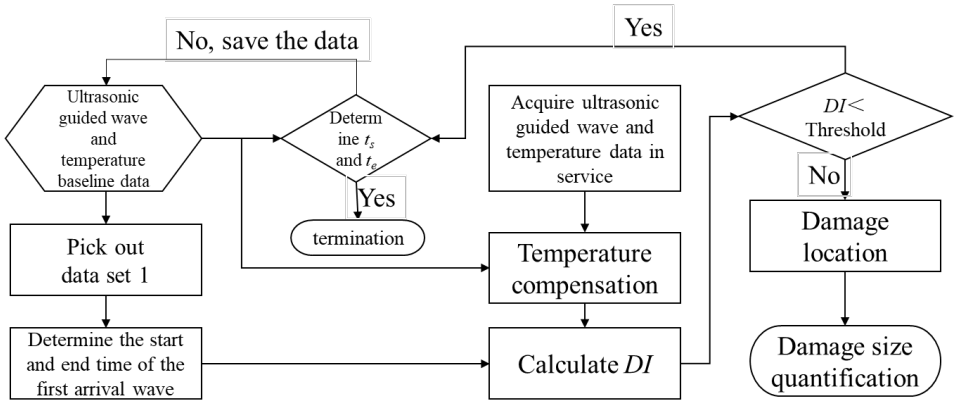


Figure 6. Data analysis process for damage diagnosis, including baseline data management

Figure 7 shows the number of piezoelectric sensors and detection paths in both monitored areas, 1 and 2. Figure 81 shows a representative example of the ultrasonic guided waveforms generated by PZT 1 (actuator) and received by PZT 4 in area 1. To reasonably determine the start and end time of the first arrival wave packet, factors such as the width of the excitation wave, the time point of the wave trough, and the noise threshold are considered. Looking specifically at the first wave packet (excluding the crosstalk), it can be concluded that the time of flight is 2.314583e-05 s. Since the center distance of the two piezoelectric ceramic plates is 68.236720 mm, the group velocity is calculated as 2948.1 m/s. The plate thickness and excitation frequency are known, and Figure 3 shows that the theoretical group velocity is 3012 m/s, so the error is 2.12%.

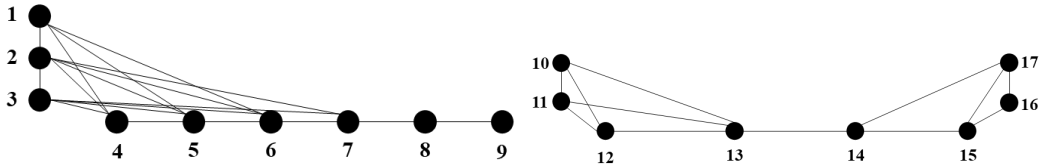


(a) monitoring area 1 (b) monitoring area 2

Figure 7. Piezoelectric sensor IDs and detection paths in monitored areas

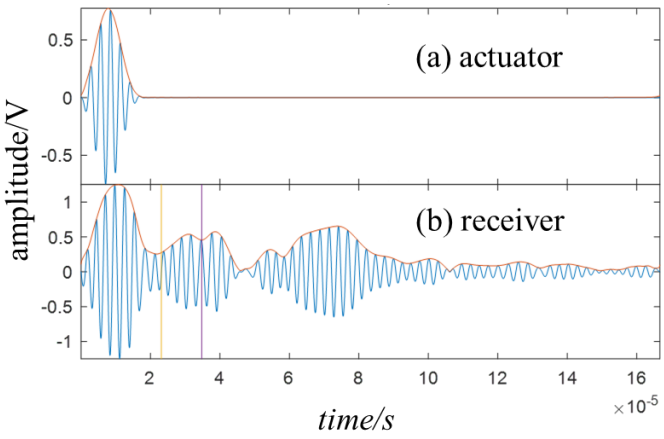


Figure 8. Ultrasonic guided wave signals from PZT 1 (actuator, a) → PZT 4 (receiver, b)

## ANALYSIS OF LINE DATA USING DAMAGE INDICES

By the end of August 2021, the onboard structural health monitoring system has been operating online for 11 months. Figure 9(a) is the train operation routing, it departs Wuhan station at 07:55 in the morning, and arrives at Shenzhenbei station after 4 hours and 47 minutes, in the afternoon, it goes from Shenzhenbei at 13:09, and arrives at Wuhan station after about 4 hours and 56 minutes, the round-trip lines are not completely coincident. As there is no damage in the structure of the train, the damage index ($DI_f$) only changes with the structural stress in the monitoring area (accompanied by noise), and daily changes are repetitive. The data of September 12th, 2020, serves as an example to analyze the $DI_f$ change law.

Figure 9(b) shows the stress distribution in the monitoring area, with the maximum tensile stress at each measuring point not exceeding 25 MPa and the maximum compressive stress not exceeding 15 MPa.

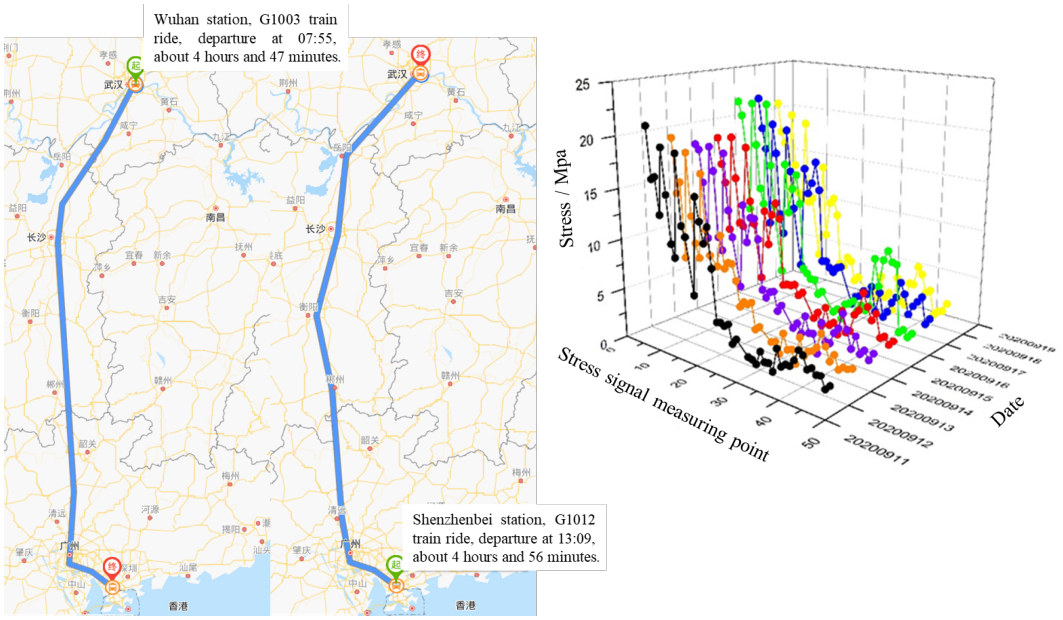


(a) (1) Wuhan to Shenzhenbei (2) Shenzhenbei to Wuhan (b) operating stress

Figure 9. The operating routes of the monitored train and operating stress of the monitored area

Figures 10 and 11 show the $DI_f$ change curves of the paths in monitoring areas 1 and 2, respectively. It can be seen from figure 10 that the $DI_f$ of path PZT 3 → PZT 6 in the monitoring area 1 reaches the maximum value at time *t1* (approximately 13:46), and, at this time, the train is running at Guangzhoubei railway station. The increased DI may be caused by the increase of the bolster weld stress caused by the influx of passengers at this station. The $DI_f$ of path PZT 2 → PZT 3 reaches its maximum value at time *t2* (approximately 14:58); at this time, the train runs between Shaoguan and Chenzhouxi. The $DI_f$ of path PZT 3 → PZT 6 peaks again at time *t3* (about 12:42), as the train runs to the vicinity of Shenzhenbei. The $DI_f$ of path PZT 2 → PZT 3 peaks at time *t4* (approximately 15:22), as the train runs between Chenzhouxi and Hengyangdong. The $DI_f$ of path PZT 12 → PZT 14 in monitoring area 2 reaches its maximum value at approximately 14:18; at this time, the train runs between Guangzhounan and Shaoguan. It is uncertain whether the DI increase is caused by the increase in passenger capacity or the poor line in this region. The $DI_f$ of path PZT 16 →

PZT 17 reaches its maximum value at about 07:22; at this time, the train is at Wuhan Station and is at a standstill. Therefore, the increase of $DI_f$ is attributed to the passenger weight causing an increase in stress.

Figures 12 and 13 show the $DI_f$ of each path in monitoring areas 1 and 2, respectively, after the train enters the warehouse. At this time, the passenger capacity is 0 and the train is at a standstill. Therefore, the influence of stress on $DI_f$ can be excluded, but the influence of noise cannot be excluded. It can be seen from the figure that $DI_f$ of path PZT 4 → PZT 9, PZT 2 → PZT 7, PZT 6 → PZT 9 in the monitoring area 1, and $DI_f$ of path PZT 12 → PZT 14 in the monitoring area 2 are larger. This is because those paths have a longer ultrasonic propagation distance and contain more environmental noise. Thus, the increase in DI on these paths cannot be used as a basis for judging damage. In addition, it can be seen from the figure that 0.08 and 0.05 are appropriate $DI_f$ thresholds for areas 1 and 2, respectively; further corrections should be made as more data is accumulated over longer periods of time.

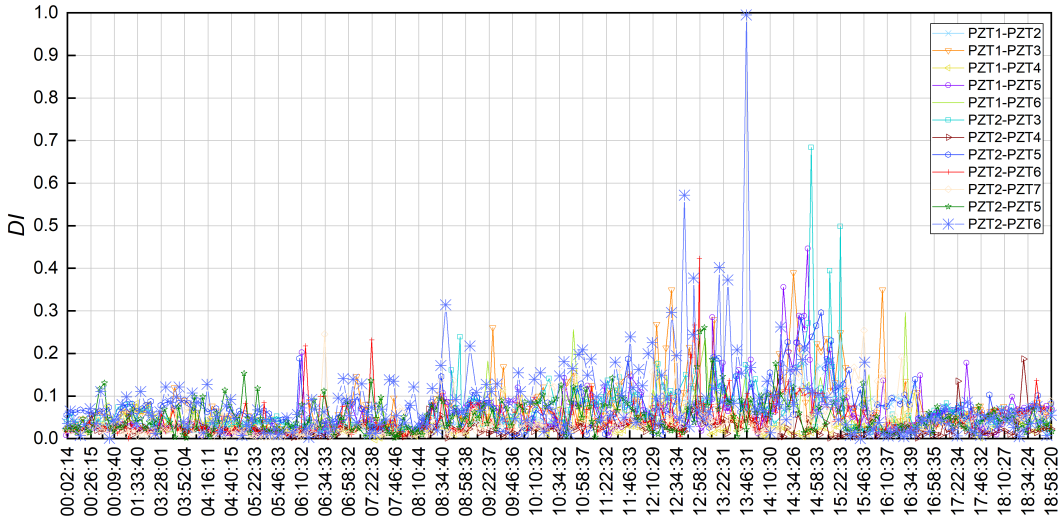


Figure 10. $DI_f$ curve in monitoring area 1

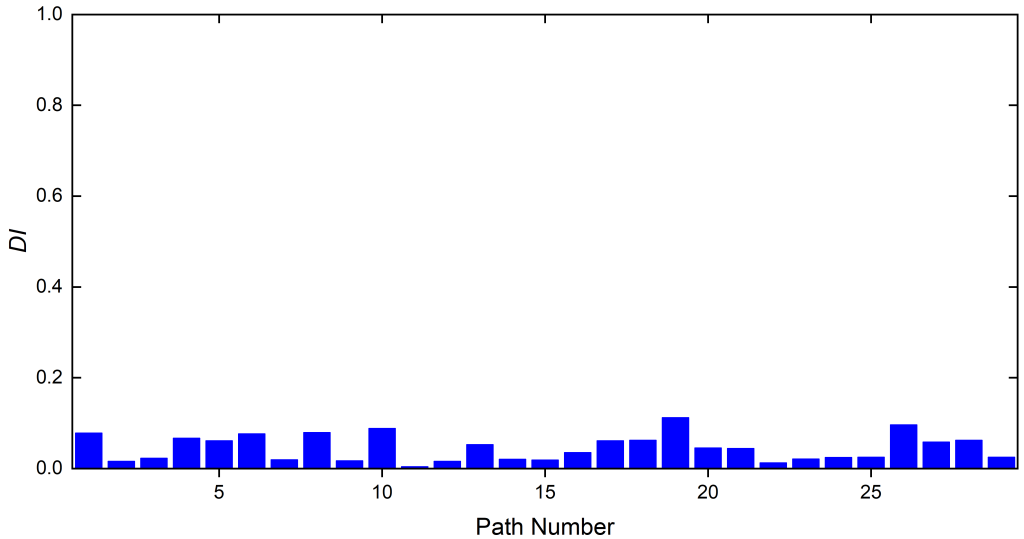


Figure 11. $DI_f$ at the last sampling time point

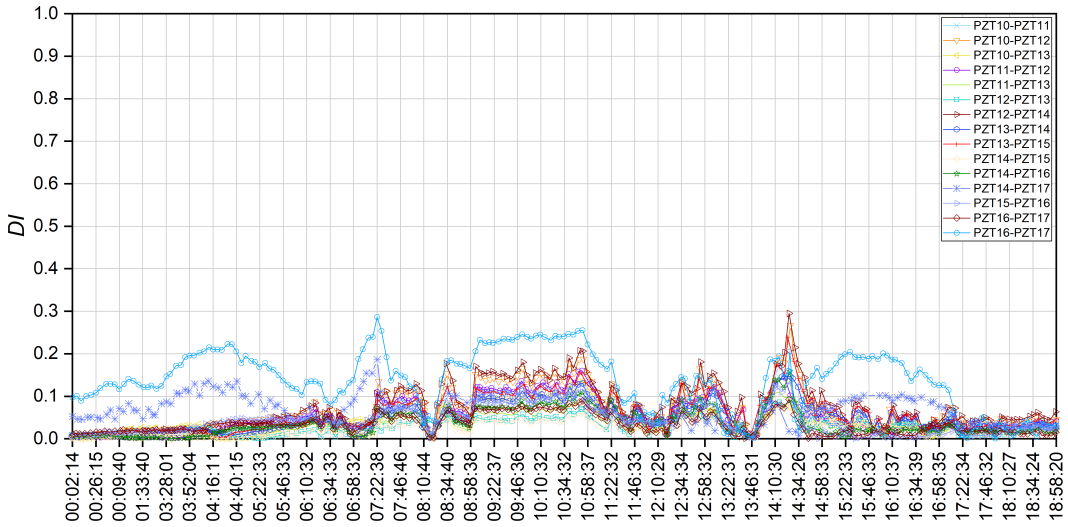


Figure 12. $DI_f$ curve in monitoring area 2

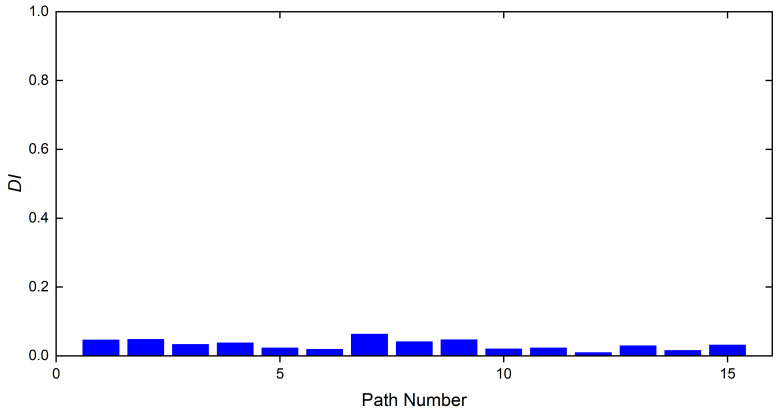


Figure 13. $DI_f$ at the last sampling time point

## CONCLUSIONS

This paper describes building and deploying a vehicle-mounted structural health monitoring (SHM) system based on piezoelectric ultrasonic guided waves, methods for managing baseline data, compensation of temperature effects, and performing damage detection analysis of real-world line test data. The results show:

(1) This SHM system can adapt to the line environment and automatically collect ultrasonic guided wave data;

(2) $DI_f$ increases according to loading conditions during operation but remains at a low level when the train enters the warehouse, making it a quantifiable indicator of damage (reasonable thresholds for the monitoring areas 1 and 2 are 0.08 and 0.05, respectively).

## REFERENCES


1. RailWorld. “China Railway Statistics Bulletin 2020 (Official data on the number of EMUs and high-speed rail operating mileage) ”, https://www.163.com/dy/article/G42R8FJQ0511T04N.html.

2. Zhang Shuguang. “Research on Design Method of High-speed Train,” *M. China Railway Publishing House*, 2009:77-108.

3. Ding Sansan, Chen Dawei, Liu jiali. 2021. “Research, Development and Prospect of China High-speed Train,” *J. Chinese Journal of Theoretical and Applied Mechanics*, 53(1): 35-50.

4. Qin Quan. 2000. *“Health monitoring of long-span bridges,” J. China Journal of Highway and Transport,* 13(2): 37-42.

5. Sun Xiasheng, Xiao Yingchun. 2014. *“Opportunities and Challenges of Aircraft Structural Health Monitoring,” J. Acta Aeronautica et Astronatucia Sinica,* 35(12): 3199-3212.

6. Qing Xinlin, Wang Yishou, Zhao Lin. 2012. *“Structural Health Monitoring Technology and Its Application in Aeronautics and Astronautics,” J. Journal of Experimental Mechanics,* 27(5): 517-526.

7. Jeong-Beom Ihn, Fu-Kuo Chang. 2004. “Detection and monitoring of hidden fatigue crack growth using a built-in piezoelectric sensor/actuator network: I. Diagnostics,” *J. Smart Mater. Struct.*, 13(2004): 609-620.

8. Zheng Yuebin, Wu Zhanjun, Lei Zhenkun, et. al. 2021. *“ Research Progress in Damage Diagnostic Imaging of Aerospace Structures Based on Ultrasonic Guided Waves,” J. Aeronautical Manufacturing Technology,* 2020, 63(18): 24-42.

9. Jianying Liang, Long Ma, Zengye Ju, et. al. 2019. “Damage assessment of high-speed EMU train axles via SHM technology based on PZT sensor networks,” presented at the 12th International Workshop on Structural Health Monitoring Structural Health Monitoring.

10. Zengye Ju, Zongzheng Wang, Long Ma. 2017. “Damage Diagnostic Techniques and Experimental Research of High-speed EMU Aluminum Carbody Bolster Based on Lamb Waves,” presented at the 11th International Workshop on Structural Health Monitoring.

11. Qiang Wang, Zhongqing Su, Ming Hong. 2014. “Online damage monitoring for high-speed train bogie using guided waves: development and validation,” presented at 7th European Workshop on Structural Health Monitoring.

12. Xiao Juncheng, Lv Pengmin, Li Fucai. 2015. “Damage Localization Imaging of Train’s Bogie Frames Based on Ultrasonic Guided Wave,” *J. Noise and Vibration Control,* 35(3): 163-168.